Journal of Alloys and Compounds 504 (2010) 192–196

Contents lists available at ScienceDirect

Journal of Alloys and Compounds

journal homepage: www.elsevier.com/locate/jallcom

High-temperature thermoelectric properties of $Ti_{0.5}(ZrHf)_{0.5-x}Nb_xNi_{0.9}Pd_{0.1}Sn_{0.98}Sb_{0.02}$ half-Heusler alloys

Ping-Jen Lee, Long-Sun Chao*

Department of Engineering Science, National Cheng Kung University, Tainan City 701, Taiwan, ROC

ARTICLE INFO

Article history:
Received 12 March 2010
Received in revised form 7 May 2010
Accepted 14 May 2010
Available online 31 May 2010

Keywords:
Half-Heusler
Thermoelectric
Seebeck coefficient

ABSTRACT

The effects of Nb substitution at the IV metal site on the thermoelectric properties of $Ti_{0.5}(ZrHf)_{0.5-x}Nb_xNi_{0.9}Pd_{0.1}Sn_{0.98}Sb_{0.02}$ half-Heusler alloy compounds were investigated by measuring the electrical resistivity, Hall effect, Seebeck coefficient and thermal conductivity. Changes in its microstructure were characterized using SEM and X-ray diffraction. It was shown that the substitution of Nb for TiNiSn-based alloys led to a significant reduction in the thermal conductivity due to the increase in defects and an enhancement of the electrical conductivity. The best sample reached a *ZT* of 0.66 at 900 K with an Nb content of $x = 0.01$.

1. Introduction

The use of half-Heusler alloys as thermoelectric materials (TE) [1] have recently been of interest due to their high thermal stability, low thermal expansion coefficient [2] and high efficiency for high temperature thermoelectric applications. The performance of thermoelectric depends on the temperature gradient (ΔT) and intrinsic material properties. The maximum efficiency is expressed as $\phi_{max} = \eta_c\gamma$, where η_c is defined by combining the Carnot efficiency $(T_H - T_C)/T_H$, and γ, which embodies the parameters of the materials $\gamma = ((\sqrt{1+ZT}-1)/(\sqrt{1+ZT}+(T_C/T_H)))$ [3]. The efficiency of energy conversion in thermoelectric materials is related to the dimensionless figure of merit ZT, which is given by $ZT = \alpha^2 T/\rho k$. A good thermoelectric material should ideally perform at a wide range of temperatures with a large Seebeck coefficient, low electrical resistivity, and low thermal conductivity. Half-Heusler semiconductors with 18 valence electrons per unit cell [4,5] possess a narrow band gap-on the order of 0.1–0.2 eV [6,7]. The associated large effective mass leads to several characteristics, which includes large thermoelectric power factors [8], large Seebeck coefficients (250 $\mu V K^{-1}$) at room temperature [9], moderate electrical resistivity (1–10 $\mu\Omega$ m) [10] and high thermal conductivity (~10 $W m^{-1} K^{-1}$) at room temperature [9]. In their efforts to achieve a higher *ZT* value, Muta et al. [11] have reported that since Nb ($4d^4 5s^1$) has an additional electron in the valence shell in comparison to Ti ($3d^2 4s^2$) and Zr ($4d^2 5s^2$), the Fermi level shifted upwards in the conduction bands. This demonstrated an enhancement of metal-like behavior in semiconductors with increasing Nb concentration. Hohl et al. [12] reported greater efficiency by doping ZrNiSn materials with Nb, which obtained a maximum power factor of 22 $\mu W cm^{-1} K^{-2}$ and low thermal conductivity of 5.2 $W m^{-1} K^{-1}$ at room temperature. Sakurada and Shutoh [13] have reported that Ti can be effectively substituted for Zr and Hf, reducing the thermal conductivity to 3 $W m^{-1} K^{-1}$. By substituting a small amount of Sb or Bi on a Sn site, or Nb or Ta on an Zr site, Hohl et al. [12] have reported a reduction in electrical resistivity without significantly decreasing the Seebeck coefficient, obtaining a power factor ($\alpha^2\sigma$) of 40 $\mu W cm^{-1} K^{-2}$ and a *ZT* value of ~0.5 at 700 K. In addition, a low thermal conductivity of 2 $W m^{-1} K^{-1}$ was reported by Shen et al. [14] in a ZrNiSn-based half-Heusler alloy, when a Ni site was substituted by Pd. Yang et al. [15] elucidated the point defect scattering for alloying Pd on the Ni sub-lattice. Other groups have investigated large concentrations of Zr ($y \geqq 25\%$) substitution at Ti sites, which reduced the thermal conductivity by mass fluctuation scattering [16]. In this work, we report the effect of substituting IV sites with Nb in $Ti_{0.5}(ZrHf)_{0.5-x}Nb_xNi_{0.9}Pd_{0.1}Sn_{0.98}Sb_{0.02}$.

2. Experimental and procedure

An ingot of the alloy $Ti_{0.5}(ZrHf)_{0.5-x}Nb_xNi_{0.9}Pd_{0.1}Sn_{0.98}Sb_{0.02}$ was made from high-purity elements (Ti (99.99%), Zr (>99.99%), Hf (>99.99%), Nb (99.95%), Ni (99.99%), Pd (99.9%), Sn (99.999%), and Sb (99.999%)) by arc melting several times to ensure homogeneity on a water cooled copper chilled under an argon atmosphere. Fig. 1 shows out the columnar dendrites and equiaxed dendrites structure by rapid solidification process which will be affect the concentration field re-distribution of element solute. The grain boundaries have more Ti-rich phase.

The samples were wrapped in tantalum foil and sealed in an evacuated quartz tube for annealing, which consisted of two stages. The first annealing was carried out for 24 h from 1173 to 1273 K to ensure homogeneity, and the second was from 970

* Corresponding author. Tel.: +886 3 5919369; fax: +886 3 5910086.
E-mail address: lschao@mail.ncku.edu.tw (L.-S. Chao).

0925-8388/$ – see front matter © 2010 Elsevier B.V. All rights reserved.
doi:10.1016/j.jallcom.2010.05.086

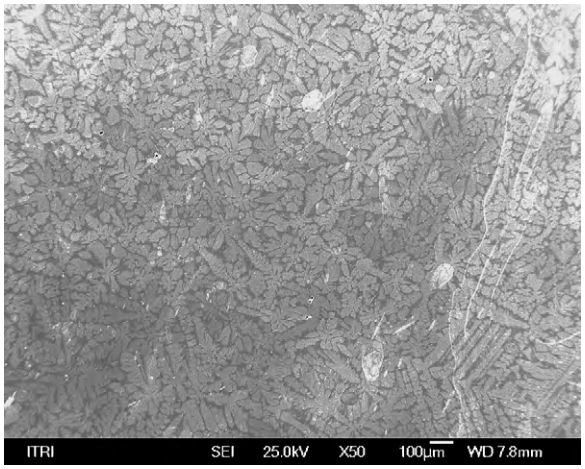

Fig. 1. The columnar dendrites and equiaxed dendrites structure by rapid solidification process.

Table 1
lattice parameters of the $Ti_{0.5}(ZrHf)_{0.5-x}Nb_xNi_{0.9}Pd_{0.1}Sn_{0.98}Sb_{0.02}$ with Nb stoichiometric concentrations, *x*.

Nb content *x*	0	0.1	0.2	0.3	0.4	0.5
Lattice (pm)	605.15	604.21	603.8	603.25	603.23	602.86

to 1070 K for 10 days to increase the ordering of the samples. Samples were taken out of the oven after annealing and cut into disks and bars. Each disk was 10 mm in diameter and 1 mm thick, whereas the bars were 3 × 3 × 12 mm. The disks and bars were used for thermal diffusion and Seebeck coefficient/resistivity measurements. The half-Heusler phase and microstructures were analyzed using X-ray diffraction (XRD), and scanning electron microscopy (SEM), respectively. In addition, the Seebeck coefficient and electrical resistivity were simultaneously measured under a He atmosphere using a ULVAC-RIKO ZEM-3 (Kanagawa, Japan). The thermal diffusivity was measured using a laser flash technique from 300 to 1000 K with ULVAC-RIKO TC-9000 in a dry nitrogen atmosphere. The specific heat capacity was measured using a Metter DSC821 with temperatures ranging from 300 to 900 K. The electrical resistivity and Hall effect was measured using a Mitsubishi MCP-T600 and Accent HL5500PC at 300 K to ensure non-crack in microstructure for thermoelectric sample.

3. Results and discussion

The effect of substituting Zr/Hf with Nb on lattice thermal conductivity was studied, while maintaining optimal Ti, Pd, and Sb concentration. The key to achieving an optimal TE figure of merit depends on many factors, and is not limited to reducing the lattice thermal conductivity. Fig. 2 shows X-ray diffraction patterns of annealed $Ti_{0.5}(ZrHf)_{0.5-x}Nb_xNi_{0.9}Pd_{0.1}Sn_{0.98}Sb_{0.02}$ (x = 0–0.05) in the range of 2θ = 20–120°. All samples were identified as half-Heusler phases by annealing from various temperatures [16]. The peak associated with the presence of impurities is visible in Ti_6Sn_5 diffraction patterns, and is essential to enhance the electronic transport properties. Table 1 shows the average lattice parameter of

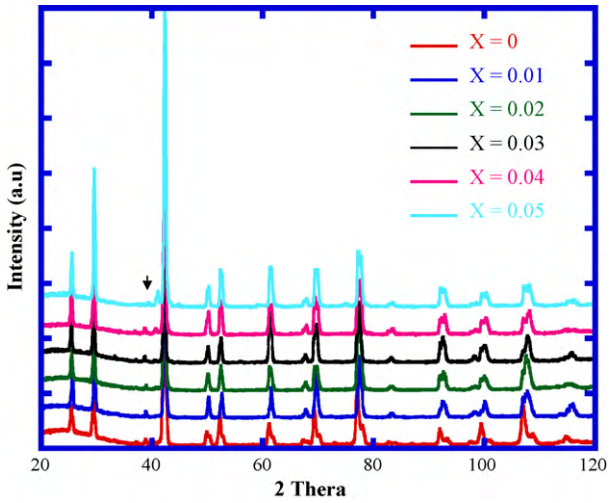

Fig. 2. X-ray diffraction patterns of $Ti_{0.5}(ZrHf)_{0.5-x}Nb_xNi_{0.9}Pd_{0.1}Sn_{0.98}Sb_{0.02}$ (x = 0–0.05) at 300 K. Asterisk indicates is Sn_5Ti_6 phase.

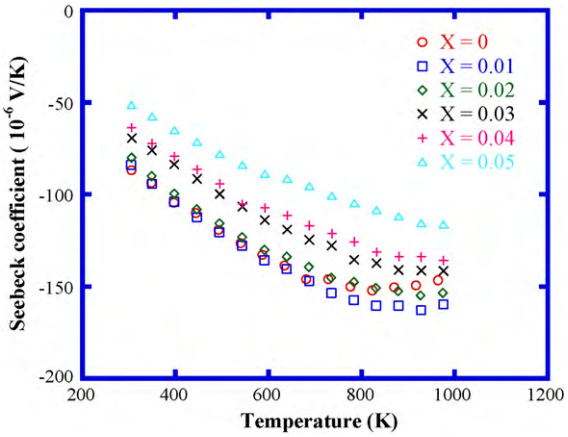

Fig. 3. Temperature dependence of the Seebeck coefficient for $Ti_{0.5}(ZrHf)_{0.5-x}Nb_xNi_{0.9}Pd_{0.1}Sn_{0.98}Sb_{0.02}$ alloys.

$Ti_{0.5}(ZrHf)_{0.5-x}Nb_xNi_{0.9}Pd_{0.1}Sn_{0.98}Sb_{0.02}$ as a function of Nb content, x. Using the XRD data (20–60°), the lattice parameters of x (x = 0–0.05) were calculated to be 6.0515, 6.0421, 6.038, 6.0325, 6.0323 and 6.0286 Å, respectively. The lattice parameter decreased linearly with increasing Nb content.

Fig. 3 shows that the absolute values of the Seebeck coefficient increased with increasing temperature in the range from 300 to 1000 K. The variation of Nb-concentration (x = 0–0.02) induced two regions at the intersection. In the first region, substitution at Zr/Hf sites with Nb at temperatures ranging from 300 to 823 K showed degenerating characteristics, where the Seebeck coeffi-

Table 2
Room temperature values of electrical transport parameters of $Ti_{0.5}(ZrHf)_{0.5-x}Nb_xNi_{0.9}Pd_{0.1}Sn_{0.98}Sb_{0.02}$ compared with Journal of Alloys and Compounds [10].

Sample	ρ (10^{-5} Ωm) ZEM	ρ (10^{-5} Ωm) Hall effect	n (10^{19}/cm^3)	μ (cm^2/V s)	α (μv/K)
$Ti_{0.99}Nb_{0.01}NiSn$ (Ref. [10])		1.23	33.0	15.0	−208.0
$Ti_{0.98}Nb_{0.02}NiSn$ (Ref. [10])		0.9174	50.0	14.0	−191.0
$Ti_{0.99}Nb_{0.01}NiSn$ (Ref. [10])		1.3158	19.0	26.0	−229.0
$Ti_{0.98}Nb_{0.02}NiSn$ (Ref. [10])		0.8929	30.0	24.0	−199.0
$Ti_{0.5}(ZrHf)_{0.5}Ni_{0.9}Pd_{0.1}Sn_{0.98}Sb_{0.02}$	0.3676	0.3777	23.7	69.9	−87.0
$Ti_{0.5}(ZrHf)_{0.49}Nb_{0.01}Ni_{0.9}Pd_{0.1}Sn_{0.98}Sb_{0.02}$	0.3532	0.3733	26.4	63.3	−83.9
$Ti_{0.5}(ZrHf)_{0.48}Nb_{0.02}Ni_{0.9}Pd_{0.1}Sn_{0.98}Sb_{0.02}$	0.3445	0.3187	33.6	58.3	−79.9
$Ti_{0.5}(ZrHf)_{0.47}Nb_{0.03}Ni_{0.9}Pd_{0.1}Sn_{0.98}Sb_{0.02}$	0.297	0.2919	37.0	57.8	−69.4
$Ti_{0.5}(ZrHf)_{0.46}Nb_{0.04}Ni_{0.9}Pd_{0.1}Sn_{0.98}Sb_{0.02}$	0.2601	0.2932	39.7	53.6	−63.7
$Ti_{0.5}(ZrHf)_{0.45}Nb_{0.05}Ni_{0.9}Pd_{0.1}Sn_{0.98}Sb_{0.02}$	0.1977	0.1841	66.4	51.1	−51.4

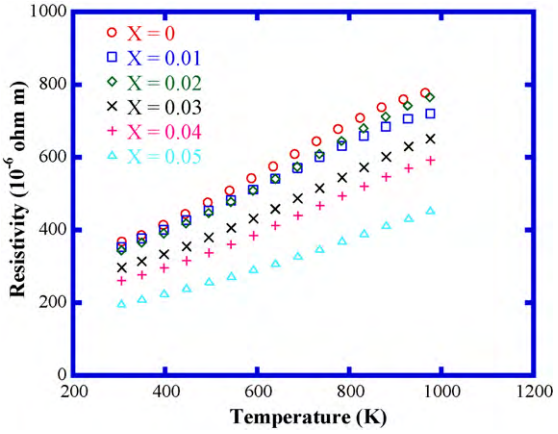

Fig. 4. The temperature dependence of electrical resistivity of $Ti_{0.5}(ZrHf)_{0.5-x}Nb_xNi_{0.9}Pd_{0.1}Sn_{0.98}Sb_{0.02}$ alloys.

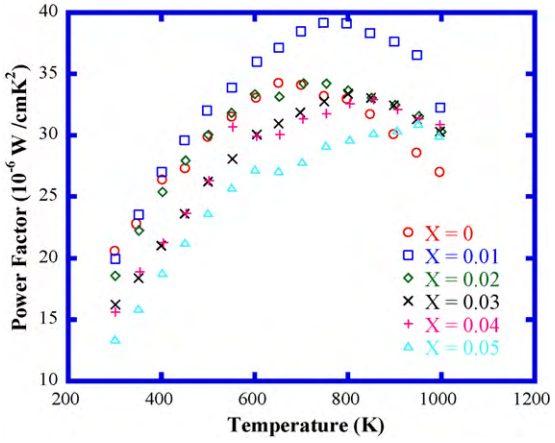

Fig. 5. Power factor of the $Ti_{0.5}(ZrHf)_{0.5-x}Nb_xNi_{0.9}Pd_{0.1}Sn_{0.98}Sb_{0.02}$ alloys as a function of temperature.

cient decreased with increasing Nb concentration. According to the Mott and John equation [17], the Seebeck coefficient of degenerated semiconductors is

$$S = -\frac{\pi^2 k_B^2 T}{3q}\frac{d\ln\sigma(E)}{dE}\bigg|_{E=E_F} \alpha -\frac{T}{N_{tot}(E)}\frac{dN_{tot}(E)}{dE}\bigg|_{E=E_F}$$

where k_B, q, $\sigma(E)$, $N_{tot}(E)$ are the Boltzmann constant, charge on an electron, electrical conductivity and value of density of state (DOS), respectively. An increase of carrier concentration from 23.7 to $66.4 \times 10^{19}/cm^3$ was observed for Nb concentrations $x = 0$–0.05 as shown in Table 2. This change in properties was believed to be caused by a shift in the Fermi-level to a higher energy in the conduction band by Nb dopants. In the second region, the absolute value of the Seebeck coefficient decreased above 823 K, which was attributed to the excitation of electron–hole pairs across the energy gap at higher temperatures, and is in agreement with the studies conducted by Hiroaki et al. [11]. Metal behavior was observed with high concentrations of Nb ($x = 0.03$–0.05) substitution at Zr/Hf sites. The Seebeck coefficient then reached a maximum of $|S| = 163\ \mu V\ K^{-1}$ with an Nb concentration of $x = 0.01$, which begins to decrease at 926 K.

Fig. 4 shows the temperature and Nb content dependence of the electrical resistivity. The electrical resistivity showed a

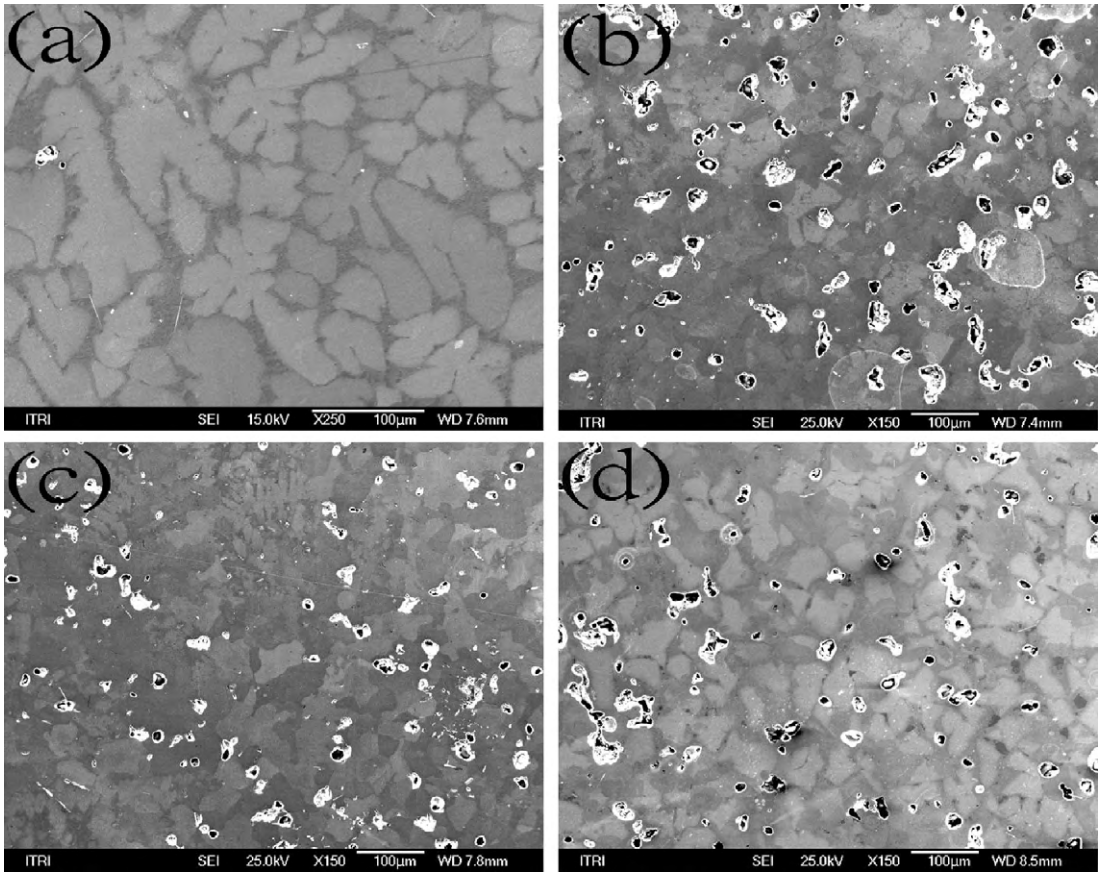

Fig. 6. SEM image the characteristic grain structure of varying sizes for $Ti_{0.5}(ZrHf)_{0.5-x}Nb_xNi_{0.9}Pd_{0.1}Sn_{0.98}Sb_{0.02}$: (a) $x = 0$, (b) $x = 0.01$, (c) $x = 0.02$ and (d) $x = 0.03$, the grain size average diameters of 20–50 μm.

slight linear decrease with increasing Nb content. Minimum carrier mobility ($\mu = 51.1\ cm^2\ V^{-1}\ s^{-1}$) with a low electrical resistivity of $0.1841 \times 10^{-5}\ \Omega m$ was achieved with an Nb concentration of $x = 0.05$, as shown in Table 2. The experimental results show that the addition of Sb is effective for the reduction of the electrical resistivity of half-Heusler alloys. Similar studies were also conducted by other groups [18–20]. In addition, doping at levels greater than 0.006 at% Sb on Sn sites results in an increase in electron carrier density [8]. Based on the Seebeck coefficient and electric conductivity results, the observed behavior showed degenerate characteristic in $Ti_{0.5}(ZrHf)_{0.5-x}Nb_xNi_{0.9}Pd_{0.1}Sn_{0.98}Sb_{0.02}$ with varying Nb concentration. Using the measured electrical resistivity and Seebeck coefficient, the power factor was calculated and is shown in Fig. 5. The power factor may be influenced by many factors such as the Fermi level [21], density of state [22], mobility (electrons and holes) [23], phonon scattering [24], and so on. From the point of electrical conductivity equation, $\sigma \sim T^{5/2} m_*^{3/2} \mu / k_{ph}$, which is a function of carrier concentration, where μ is carrier mobility, m^* is carrier effective mass, and k_{ph} is lattice thermal conductivity. In order to achieve better thermoelectric performance, a higher mobility to thermal conductivity ratio is required. In this study, the highest power factor was achieved when the Nb concentration was in the range $x = 0$–0.05. The power factor was observed to reach ~39.18 $\mu W\ cm^{-1}\ K^{-2}$ at 800 K with larger mobility ($63.9\ cm^2/V\ s$) when Nb substitution level $x = 0.01$. The results yielded consistent with the electrical conductivity equation. It is believed that this might be either a change in electronic band structure, or doping the compound using Sb and Nb due to the V and Sb have one more electron and enhance the carrier mobility.

Fig. 6(a)–(d) shows the SEM image with different Nb concentrations, with x ranging from 0 to 0.03. Intuitively, the grain size decreased and voids increased with increasing Nb concentration. Both the grain size and voids influence the thermal conductivity. It appears that the sample readily formed voids with increased Nb-doping, which leads to phonon scattering, reducing thermal conductivity. The total thermal conductivity as a function of temperature for the series $Ti_{0.5}(ZrHf)_{0.5-x}Nb_xNi_{0.9}Pd_{0.1}Sn_{0.98}Sb_{0.02}$ ($x = 0$–0.05) is shown in Fig. 7. It demonstrates that the thermal conductivity slightly increased with increasing Nb substitution from $x = 0$ to $x = 0.05$. According to the Wiedmann–Franz–Lorenz Law, $L = (k/\sigma T) = (\pi^2/3)(k_B/e)^2 T$, where L is the Lorenz number and is characterized by σ and k, respectively, the thermal conductivity is proportional to electrical conductivity at constant temperature. The behavior of thermal conductivity agrees with the trend of electrical conductivity.

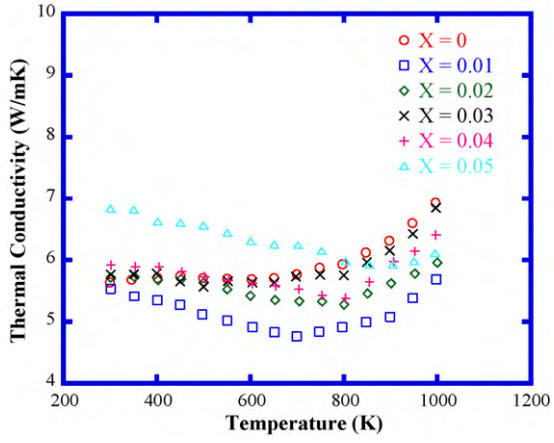

Fig. 7. The effect of (ZrHf) alloying at the Nb site on the thermal conductivity of $Ti_{0.5}(ZrHf)_{0.5-x}Nb_xNi_{0.9}Pd_{0.1}Sn_{0.98}Sb_{0.02}$ alloys as a function of temperature.

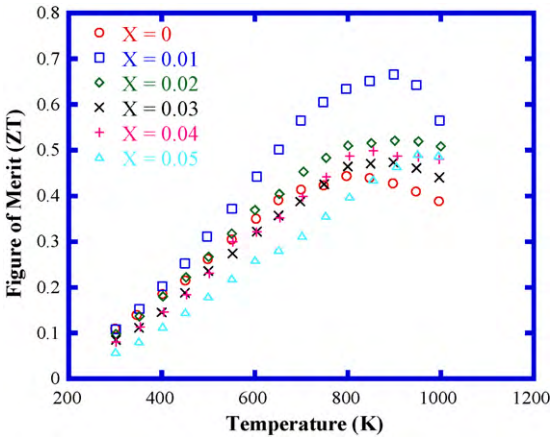

Fig. 8. Thermoelectric figure of merit for (ZrHf) alloying at the Nb site as a function of temperature.

Fig. 8 shows the dimensionless figure of merit, ZT, for all samples from 300 to 900 K. Nb substitution in the compound $Ti_{0.5}(ZrHf)_{0.5-x}Nb_xNi_{0.9}Pd_{0.1}Sn_{0.98}Sb_{0.02}$ was observed to reduce thermal conductivity ($4.75\ W\ m^{-1}\ K^{-1}$) and enhance the power factor ($38.47\ \mu W/cm\ K^2$). When Nb substitution concentrations reaches $x = 0.01$, the ZT value reached ~0.66 at 900 K.

These results demonstrate that the presence of Nb can lead to voids in alloys that possess a NiSn phase, which reduces the total thermal conductivity and enhances the ZT value in relatively high temperature ranges.

4. Conclusions

The effect of Nb substitution on the high temperature thermoelectric properties of $Ti_{0.5}(ZrHf)_{0.5-x}Nb_xNi_{0.9}Pd_{0.1}Sn_{0.98}Sb_{0.02}$ compounds was systematically studied. Alloying by Nb substitution into Zr and Hf sites led to an increase in the power factor, achieving a maximum value of $39.18\ \mu W/cm\ K^2$ at 800 K and Nb content $x = 0.01$. It demonstrated a degenerative effect in $Ti_{0.5}(ZrHf)_{0.5-x}Nb_xNi_{0.9}Pd_{0.1}Sn_{0.98}Sb_{0.02}$ with Nb concentration. The total thermal conductivity increased slightly with increasing Nb substitution from $x = 0$ to $x = 0.05$. The sample readily formed voids in the NiSn phase with increasing Nb-doping, leading to phonon scattering, and consequently reducing the thermal conductivity. Finally, a ZT value of 0.66 at 900 K was obtained for $Ti_{0.5}(ZrHf)_{0.49}Nb_{0.01}Ni_{0.9}Pd_{0.1}Sn_{0.98}Sb_{0.02}$ alloys.

Acknowledgement

The work was supported by the National Science Council of Taiwan, Republic of China under contract no. NSC-98-2221-E-006-230. One of authors (P. J. Lee) would like to acknowledge Dr. Chou of the Energy and Environment Research Laboratories, ITRI for the assistance in measurement Seebeck coefficient.

References

[1] W. Jeitschko, Metall. Trans. A 1 (1970) 3159.
[2] D.Y. Jung, K. Kurosaki, C.E. Kim, H. Muta, S. Yamanaka, J. Alloys Compd. 489 (2010) 328–331.
[3] D.M. Rowe, Thermoelectric Hand Book: Marco to Nano, pp. 4–5 (Chapter 1).
[4] J. Tabola, J. Peirre, J. Alloys Compd. 296 (2000) 243.
[5] S.J. Poon, in: T.M. Tritt (Ed.), Recent Trends in Thermoelectric Materials Research. II. Semiconductors and Semimetals, vol. 70, Academic Press, New York, 2001, pp. 37–76.
[6] F.G. Aliev, N.B. Brandt, V.V. Moshchalkov, V.V. Kozyrkov, R.V. Skolozdra, A.I. Belogorokhov, Phys. B: Condens. Matter 75 (1989) 167.
[7] B.A. Cook, J.L. Harringa, Z.S. Tan, W.A. Jesser, Proceedings of the 15th International Conference on Thermoelectrics, Istanbul, Turkey, 1996, p. 122.

[8] C. Uher, J. Yang, S. Hu, D.T. Morelli, G.P. Meisner, Phys. Rev. B 59 (1999) 8615–8621.
[9] Terry M. Tritt, S. Bhattacharya, Y. Xia, V. Ponnambalam, S.J. Poon, N. Thadhani, Appl. Phys. Lett. 81 (1) (2002) 43.
[10] G.S. Nolas, S.J. Poon, M. Kanatzidis, MRS Bull. 31 (2006) 201.
[11] H. Muta, T. Kanemitsu, K. Kurosaki, S. Yamanaka, J. Alloys Compd. 469 (2009) 50–55.
[12] H Hohl, A.P. Ramirez, C. Goldmann, G. Ernst, B. Wolfing, E. Bucher, J.Phys.: Condens. Matter 11 (1999) 1697–1709.
[13] S. Sakurada, N. Shutoh, Appl. Phys. Lett. 86 (2005) 2105.
[14] Q. Shen, L. Chen, T. Goto, T. Hirai, J. Yang, G.P. Meissner, et al., Appl. Phys. Lett. 79 (2001) 4165.
[15] J. Yang, G.P. Meisner, L. Chen, Appl. Phys. Lett. 85 (7) (2004) 1140–1142.
[16] S. Bhattacharya, M.J. Slove, M. Russell, T.M. Tritt, Y. Xia, V. Ponnambalam, S.J. Poon, N. Thadhani, Phys. Rev. B 77 (2008) 184203.
[17] R.D. Baranard, The Theory of the Properties of Metals and Alloys, Dover, New York (1972).
[18] N. Shutoh, S. Sakurada, J. Alloys Compd. 389 (2005) 204–208.
[19] S. Bhattacharya, A.L. Pope, R.T. Littleton, I.V. Terry, M. Tritt, V. Ponnambalam, Y. Xia, S.J. Poon, Appl. Phys. Lett. 77 (13) (2000) 2476–2478.
[20] S.R. Culp, S.J. Poon, N. Hickman, Terry M. Tritt, J. Blumm, Appl. Phys. Lett. 88 (2006) 042106.
[21] B. Partoens, F.M. Peeters, Phys. Rev. B 74 (2006) 075404.
[22] Hick, Dresselhaus, Phys. Rev. B 47 (1993) 12727.
[23] C. Yu, L. Shi, Z. Yao, D. Li, A. Majumdar, Nano Lett. 5 (2005) 1842.
[24] M.S. Dresslhaus, G. Dresselhaus, P. Avouris, Carbon Nanotube: Synthesis, Structure, Properties, and Application, Springer, Berlin, 2001.